3Pb2-1

Proceedings of Symposium on Ultrasonic Electronics, Vol. 33 (2012) pp. 425-426
13-15 November, 2012

Modified image reconstruction technique for ultrasonic TOF-CT

超音波音速 CT における画像最構成手法の改良

Hiroya FUJII1[1†], Kazunari ADACHI[1], Hirotaka YANAGIDA[1], Tomoki HOSHINO[1], Tomoya NISHIWAKI[2] ([1] Graduate School of Sci. and Eng. Yamagata Univ.; [2]Graduate School of Eng. Tohoku Univ.)

藤井 尋也[1†], 足立 和成[1], 柳田 裕隆[1], 星野 智紀[1], 西脇 智哉[2] ([1]山形大院 理工, [2]東北大院 工)

1. Introduction

Figure 1 illustrates the concept of ultrasonic time-of-flight computed tomography (TOF-CT) system. In the TOF-CT system, ultrasonic longitudinal wave pulses emitted from the transmitter placed on the circumference of the cross section of the object to be inspected propagate to the receiver also on the circumference. The values of TOF of the pulses are measured for many propagation paths, and the measured data are incorporated into some projected TOF profiles by means of interpolations. Finally, a cross-sectional image of the object is reconstructed from the profiles as a distribution of relative slowness of sound using the filtered back-projection (FBP) algorithm[1].

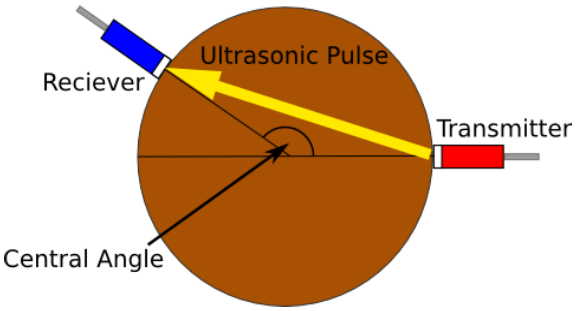

Fig. 1 Ultrasonic TOF-CT System.

As a new technique to determine the TOF for the ultrasonic CT, we previously proposed the method called the 'squared-amplitude integral method'[2]. In the numerical simulations, we found that this method can provide fine CT images more easily than conventional ones. Nevertheless, it has not been experimentally confirmed yet. In the present study, we examine the validity of this method through experiments of cross-sectional imaging of a cylindrical mortal specimen.

2. Mortar specimen and experiment

Figure 2 shows the mortar specimen without anomaly inside for the TOF-CT experiment. The cross-sectional image of the specimen was reconstructed from the data of TOF determined by the squared-amplitude integral method with the use of the TOF-CT system. The period of time during which the squared amplitude of received ultrasonic signal was integrated, or the 'window time,' was set at 290 μs. The threshold level of the integrated value of the squared amplitude for determination of the arrival time of the signal was set at 0.003% of its total integrated value for the whole window time considering attenuation of ultrasonic pulse in the specimen. **Figure 3** shows the reconstructed CT image in which significant concentric circular artifacts appear unlike that previously obtained in the simulation.

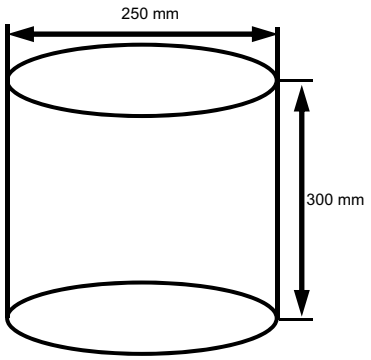

Fig. 2 Mortar specimen for the TOF-CT experiment.

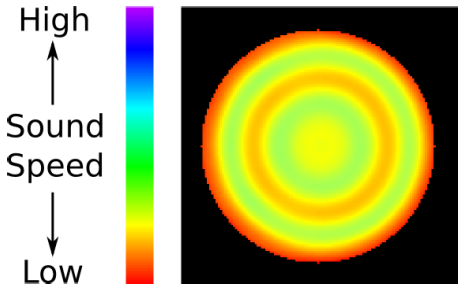

Fig. 3 TOF-CT image of the mortar specimen.

3. Comparison between the simulated results and experimental ones

We conducted simulation of wave propagation in the specimen using the material constants obtained by its uniaxial compression test in order to identify differences between the actual measurement and the

simulation. In the simulation, attenuation of ultrasonic pulse was not taken into account.

Figure 4 shows the integrated squared amplitude of the received ultrasonic signal obtained in the simulation (a) and the experiment (b). On comparison, large difference in the rise time of the received signals is observed in the range of the central angle of propagation path from 20 to 100 degrees.

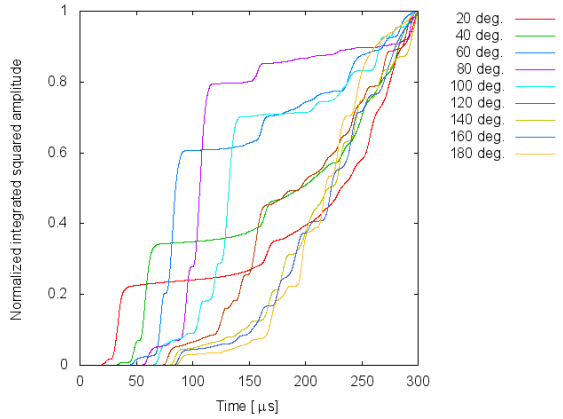

(a) Simulation

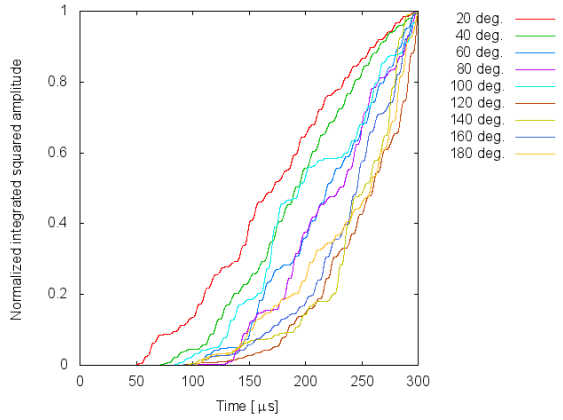

(b) Experiment

Fig. 4 Integrated squared amplitude of the received signal as functions of time in the simulation and the experiment.

In the simulation, propagation speed of the elastic wave suggests that the steep rise of the received signal can be attributed to arrival of large surface wave. On the other hand, in the experiment, such abrupt rise of the received signal was not observed.

Let us consider the reason why the large surface wave seen in the simulation was not observed in the experiment. The difference in wavelength due to wave type should be the most crucial factor. In the following equations, λ_l and λ_{saw} are the wavelengths of surface and longitudinal waves respectively in the medium.

$$\lambda_l = \sqrt{\frac{E}{\rho}} \Big/ f \qquad \textbf{(1)}$$

$$\lambda_{saw} \approx 0.9 \cdot \sqrt{\frac{G}{\rho}} \Big/ f \qquad \textbf{(2)}$$

where $E = 13.91 \times 10^9$ is Young's modulus, ρ =2157 kg/m^3 density, $\nu = 0.3$ Poisson's ratio, G = 5.3 $\times 10^9$ shearing modulus, f = 68.5 kHz the resonance frequency of the identical transducers used in the transmitter and the receiver.

The diameter of the circular receiving face of the receiver is 20 mm. The wavelength of surface wave λ_{saw} is approximately 20 mm at the frequency whereas that of the longitudinal wave λ_l is 37 mm. Thus, the diameter of the receiving face is almost equal to the wavelength of surface wave. Since the output voltage of the receiver is proportional to the average of vibration velocity on the receiving face, the surface wave was not detected but the longitudinal one was in the experiment.

4. Conclusion

In the present study, we prepared a mortar specimen of 250 mm in diameter and measured the values of TOF of ultrasonic pulses for many propagating paths in its uniform cross section. The TOF was determined by the squared-amplitude integral method previously proposed by us. However, the uniform reconstructed image obtained in the simulation could not be observed in the experiment.

The artifacts visualized as slowness parts in the reconstructed TOF-CT image have previously been considered due to large surface waves whose propagation speed is lower than longitudinal wave to be detected. Nevertheless, such large surface wave could not actually be detected in the received signal for the mortar specimen because of its wavelength almost the same as the diameter of the receiving face of the receiver. Hence, the artifacts cannot be ascribed to the influence of surface wave in this case. It may, therefore, be inevitable to set different threshold value of the signal to determine TOF for each propagation path depending on the its central angle so as to obtain appropriate TOF-CT images in its actual applications.

References

1. K. Adachi *et.al.*, Journal of Archaeological Prospection Society of Japan, **12** (2010) 47-56 [In Japanese].
2. H. Fujii and K. Adachi. Reports of the 2012 spring meeting the Acoustical Society of Japan. (2012) 1421-1424 [In Japanese].